Supporting Information of

Enhanced photocatalytic H_2O_2 yield by single-atom Pt decorated carbon nitride sheets *via* boosting *OOH intermediate generation

Jinghua An[1], Zhaohui Wang[1], Guanyun Liu[1], Lu Li[1,*], and Bo Tang[1,2]

[1] College of Chemistry, Chemical Engineering and Materials Science, Key Laboratory of Molecular and Nano Probes, Ministry of Education, Collaborative Innovation Center of Functionalized Probes for Chemical Imaging in University of Shandong, Institute of Molecular and Nano Science, Shandong Normal University, Jinan, 250014, China.

[2] Laoshan Laboratory, 168 Wenhai Middle Rd, Aoshanwei Jimo, Qingdao 266237, Shandong.

* Corresponding author E-mail: lilu5252@163.com. Tel: +86 15954911357.

1. Materials and Methods

1.1 Materials

All reagents were commercially obtained and used without further purification.

Chemicals	Purity	Corporation
$H_2PtCl_6·6H_2O$	35.0-38.0 % metal basis	The Non-Ferrous Metal Institute of Shenyang, China
melamine	99%	Shanghai Macklin Biochemical Co.,Ltd (Shanghai,China)
glycerol	≥99.7%	Sinopharm Chemical Reagent Co., LTD. (Shanghai, China)
ethanol	≥99.7%	Sinopharm Chemical Reagent Co., LTD. (Shanghai, China)
phosphorous acid	85-90%	Shanghai Aladdin Biochemical Teachnology Co.,Ltd. (Shanghai,China)
O_2	≥99.5%	Jinan Deyang Special gas Co., LTD. (Jinan,China)
N_2	≥99.5%	Jinan Deyang Special gas Co., LTD. (Jinan,China)
CO	99.9999%	Dalian Institute of Chemical Physics, Chinese Academy of Sciences, China
isopropanol	≥99.5%	Shanghai Macklin Biochemical Co.,Ltd. (Shanghai,China)
$HAuCl_4·3H_2O$	99.99%	Sigma Aldrich
trisodium citrate	99%	Alfa Aesar
acetone	≥99.7%	Yantai Far East Fine Chemical Co., LTD
benzoquinone (PBQ)	99%	Shanghai Macklin Biochemical Co.,Ltd. (Shanghai,China)
(3-aminopropyl) trimethoxysilane	97%	Alfa Aesar

(APTMS)		
barium sulfate	≥99.7%	Shanghai Aladdin Biochemical Teachnology Co.,Ltd. (Shanghai,China)
Na_2SiO_3	99%	Sigma Aldrich
KBr	99.9%	Shanghai Macklin Biochemical Co.,Ltd. (Shanghai,China)
5wt% nafion ethanol solution	Volatile organic compounds content:50±3% Exchange capacity：1.03-1.12 Resin content：5%	Cool chemical science and technology. (Beijing,China)
$K_4[Fe(CN)_6]$	99%	Shanghai Macklin Biochemical Co.,Ltd. (Shanghai,China)
L-tryptophan	99%	Shanghai Aladdin Biochemical Teachnology Co.,Ltd. (Shanghai,China)
KI	≥99.0%	Shanghai Aladdin Biochemical Teachnology Co.,Ltd. (Shanghai,China)
$(NH_4)_6Mo_7O_{24}$ $4H_2O$	≥99.7%	Shanghai Macklin Biochemical Co.,Ltd. (Shanghai,China)
purified water	100%	Hangzhou Wahaha Group (Zhejiang, China)

1.2 Catalyst preparation

Preparation of bulk g-C_3N_4.

The bulk g-C_3N_4 was prepared by a calcined method. Briefly, 10 g melamine was put into a ceramic crucible, and placed it in muffle furnace. The melamine was calcined at 520 ºC in air atmosphere for 4 h with a ramp rate of 2.5 ºC·min^{-1}. Finally, a yellow g-C_3N_4 was obtained.

Preparation of g-C_3N_4 sheets. The g-C_3N_4 sheets was prepared by a facile molecule self-assembly strategy.[1] 1 g melamine and 1.2 g phosphorous acid were poured in 100 ml deionized (DI) water and stirred at 80 ºC for 1 hour. Then, the mixture was transferred to Teflon bottle. The Teflon bottle was subsequently inserted into an autoclave and subjected to hydrothermal treatment at 180 °C for 10 h in oven. After cooling, the white precipitate was separated by centrifugation and washed repeatedly with DI water, followed by drying in an oven overnight at 60 °C. After that, 0.6 g white precipitate was dispersed in a mixture solution containing 5 mL glycerol and 15 mL anhydrous ethanol. The mixture solution refluxed at 90 ° C for 3 h. After cooling, the precipitate was separated by centrifugation and washed repeatedly with ethanol, followed by drying in an oven overnight at 60 °C. Then, the precipitate was calcined at 450 ºC for 2 h with a ramp rate of 4.0 ºC·min^{-1} under Ar atmosphere. Finally, a light-yellow sample was obtained and marked as g-C_3N_4 sheets.

Preparation of Pt-SA/g-C_3N_4 sheets. Briefly, 0.6 g of white precipitate, obtained from the preparation of g-C_3N_{4-x} sheet, was dispersed in a mixture solution containing 5 mL glycerol and 15 mL anhydrous ethanol, as well as certain amount of $H_2PtCl_6 \cdot 6H_2O$. The mixture solution refluxed at 90 ° C for 3 h. After cooling, the precipitate was separated by centrifugation and washed repeatedly with ethanol, followed by drying in an oven overnight at 60 °C. Then, the precipitate was calcined at 450 ºC for 2 h with a ramp rate of 4.0 ºC·min^{-1} under Ar atmosphere. Finally, a light-yellow sample was obtained and marked as Pt-SA/g-C_3N_4 sheets.

1.3 Catalytic reactions

Photocatalytic reactions. Photocatalytic reactions were conducted in a photoreactor (100 mL). Briefly, 20 mg catalyst, 20 mL DI water, 2 mL isopropanol and magnetic bar were added into the quartz reaction tube, followed by replacing the atmosphere by O_2 for 30 min. Then, reaction mixture was stirred for another 30 min under dark with continuous oxygen supply. After that, the photocatalytic oxygen reduction reaction was conducted under the illumination of a 6 W blue LED (455 ± 5 nm) light. After irradiation for the desired time, the H_2O_2

concentration was quantitatively analyzed using iodometry method.[2] Briefly, 50 μL solution obtained after reaction was mixture with 2.0 mL 0.1 M KI aqueous solution, 0.05 mL 0.01 M $(NH_4)_6Mo_7O_{24}$ $4H_2O$ aqueous solution and reacted for 15 min under static state. During this process, the H_2O_2 in the solution obtained after reaction can react with I^{-1} to produce I_3^{-1}. And the obtained I_3^- have a typical absorption peak at 351 nm. Then, the amount of H_2O_2 could be calculated based on the typical absorption peak intensity of I_3^-, which can be measured using ultraviolet visible spectroscopy.

The H_2O_2 decomposition experiments. The H_2O_2 decomposition experiments were implemented to evaluate its stability under a photocatalytic system. Generally, the mixture solution of H_2O_2 (1 mM, 20 mL) and photocatalysts (1 mg mL^{-1}) were ultrasonicated sufficiently to obtain a uniform system. Then, open the light source and measure the concentrations of remaining H_2O_2 every 1 h to detect its stability.

Active oxygen species trapping experiment. The active oxygen species trapping experiment in the photocatalytic oxygen reduction reaction was trapped *in situ* by p-benzoquinone (PBQ) or L-tryptophan. This procedure is similar with the procedure of photocatalytic reactions except for the addition of p-benzoquinone (PBQ) or L-tryptophan.

Fluorescence capture experiment of singlet oxygen. Single oxygen sensor green (SOSG), a high specific fluorescent probe of $^1O_2$, was used to detect the generation of $^1O_2$.[3] Briefly, 2 mL DI water, 0.2 mL isopropanol, 5 μM SOSG, and 2 mg catalyst (g-C_3N_4 sheets or Pt-SA/g-C_3N_4 sheets) were added into the quartz reaction tube, followed by replacing the atmosphere by O_2 for 30 min. Then, reaction mixture was treated with 455 nm LED illumination for 4 min continuously. The fluorescence intensity was collected every 1 min. Each spectrum was recorded at room temperature.

1.4 Catalyst characterizations

The atomic resolution microscopy analysis was performed on a JEM ARM200F thermal-field emission microscope with a probe spherical aberration (Cs) corrector working at 200 kV. The transmission electron microscopy (TEM) was carried out on a Hitachi HT7700 transmission electron microscope (JEOL Ltd, Japan). The high-resolution transmission electron microscopy (HRTEM) was performed on a JEOL JEM-2100 electron microscope operating with a LaB6 cathode and an acceleration voltage of 200 kV. Compositional maps were obtained with energy-dispersive X-ray spectroscopy (EDX) using four large-solid-angle symmetrical Si drift detectors.

The atomic force microscopy (AFM) image was obtained from a Cypher VRS AFM (Oxford Instruments) under tapping mode by using an AC240TS probe at a scan rate of 2.44 Hz.

The powder X-ray diffraction (XRD) patterns of the catalysts were performed on a Smart Lab Se (Rigaku, Japan). Continuous scans were collected in the 2θ range of 10–80°. X-ray photoelectron spectroscopy (XPS) analyses were performed on a VGESCALAB MKII X-ray photoelectron spectrometer with an excitation source of Mg Kα = 1253.6 eV. The UV-vis absorption spectra of the samples were obtained with a Hitachi U-3010 UV-vis spectrophotometer (JEOL Ltd, Japan) with $BaSO_4$ as the reference. Electron paramagnetic resonance (EPR) was measured on Bruker-A200. The content of the Pt in Pt-SA/g-C_3N_4 was tested by the inductively coupled plasma optical emission spectrometry (ICP-OES). The steady photoluminescence (PL) spectra were determined by an Edinburgh Instruments FLS1000 under 365 nm excitation at room temperature.

The electrochemical measurements of the powdery samples (bulk g-C_3N_4, g-C_3N_4 sheets, and Pt-SA/g-C_3N_4 sheets) were carried out using a three-electrode system at an electrochemical station (CHI660E), where a sample-coated FTO glass electrode was used as the working electrode, a platinum gauze was used as the counter electrode, and a Ag/AgCl electrode was selected as the reference electrode. The working electrode was prepared as follows: 10 mg catalyst was dispersed in 1 mL of ethanol containing 50 μL 5wt% Nafion solution. After the

mixture was sonicated for 30 min to a homogeneous suspension, it was dropped onto a clean FTO glass. The FTO glass was dried at RT for 1 h and a uniform electrode was obtained.

1.5 Density functional theory (DFT) calculations

All the calculations are performed in the framework of the density functional theory with the projector augmented plane-wave method, as implemented in the Vienna ab initio simulation package.[4] The generalized gradient approximation proposed by Perdew, Burke, and Ernzerhof is selected for the exchange-correlation potential.[5] The long range van der Waals interaction is described by the DFT-D3 approach.[6] The cut-off energy for plane wave is set to 400 eV. The energy criterion is set to 10^{-5} eV in iterative solution of the Kohn-Sham equation. A vacuum layer of 15 Å is added perpendicular to the sheet to avoid artificial interaction between periodic images. The Brillouin zone integration is performed using a 3×3×1 k-mesh. All the structures are relaxed until the residual forces on the atoms have declined to less than 0.03 eV/Å. The free energy of each elementary step is estimated at T=298 K according to the following formula:

$$\Delta G=\Delta E+\Delta ZPE-T\Delta S$$

Where ΔE is the energy calculated using DFT. ΔZPE and ΔS are the differences in zero-point energy and entropy, respectively, between the adsorbed species and the gas phase molecules.

2. Supplementary figures (Figure S1-Figure S7)

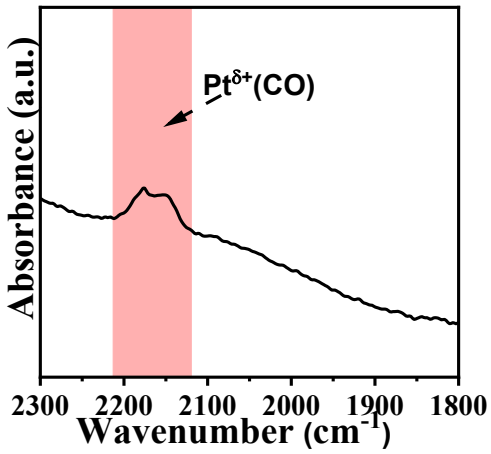

Figure S1. The CO-adsorption IR spectra of Pt-SA/g-C_3N_4.

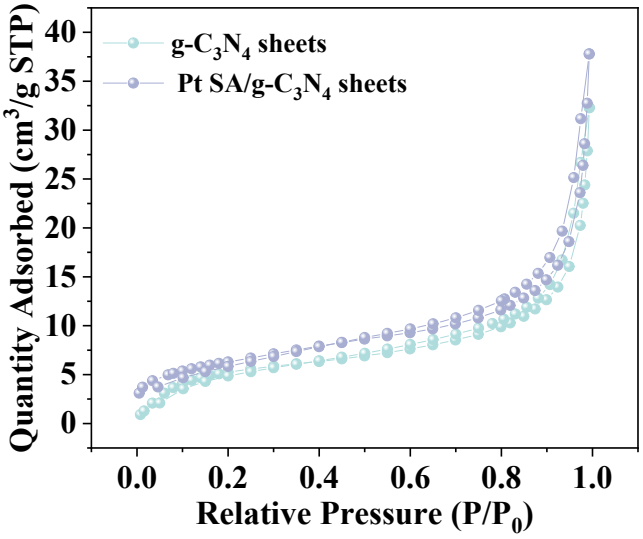

Figure S2. Nitrogen gas adsorption and desorption isotherms of g-C_3N_4 sheets and Pt-SA/g-C_3N_4 sheets.

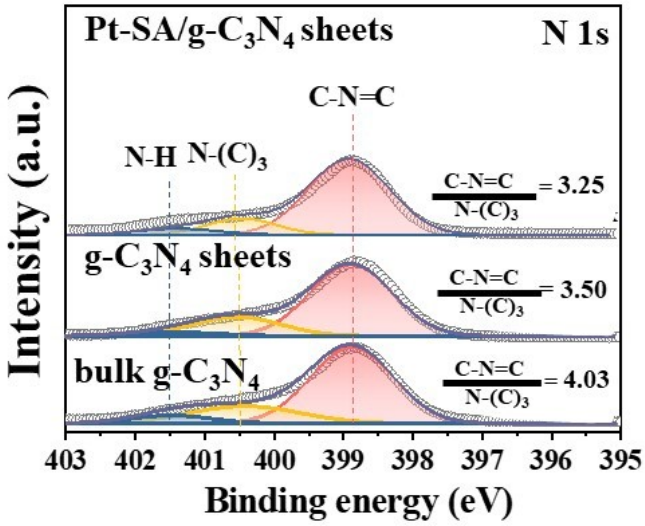

Figure S3. N 1s XPS spectra of g-C3N4, g-C3N4 sheets, and Pt-SA/g-C3N4 sheets.

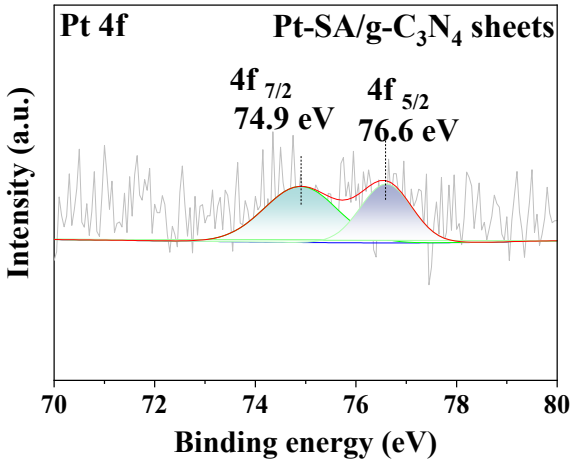

Figure S4. High-resolution XPS of Pt in Pt-SA/g-C_3N_4 sheets.

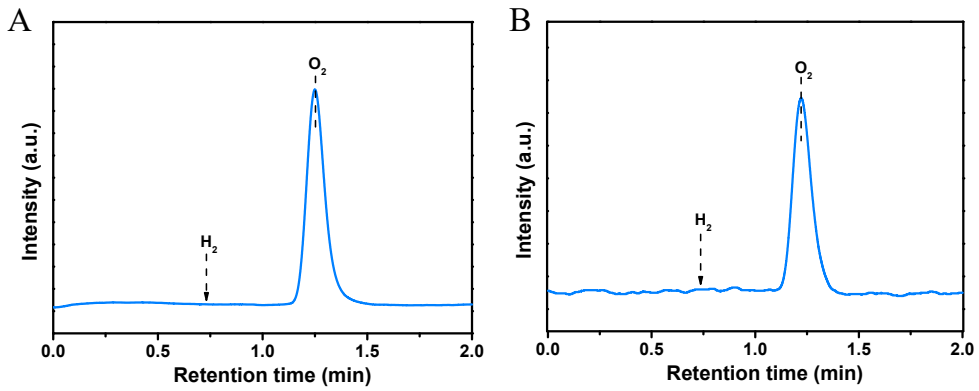

Figure S5. GC spectra over the reaction time. (A) Pt-SA/g-C_3N_4 sheet was used as a catalyst. (B) g-C_3N_4 sheet was used as a catalyst. Conditions: 20.0 mg of photocatalyst, 20.0 mL of O_2 saturation water, isopropanol (10 vt %), 6 W blue LEDs (455 ± 5 nm), RT, 4 h.

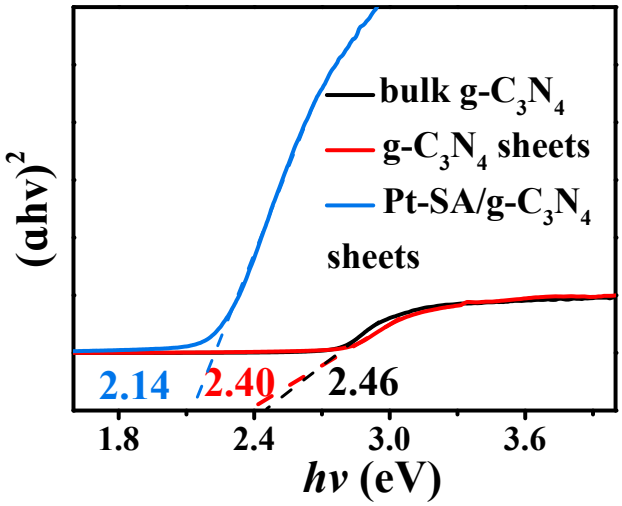

Figure S6. The plots of $(ahv)^2$ vs the energy of absorbed light in Figure 4a.

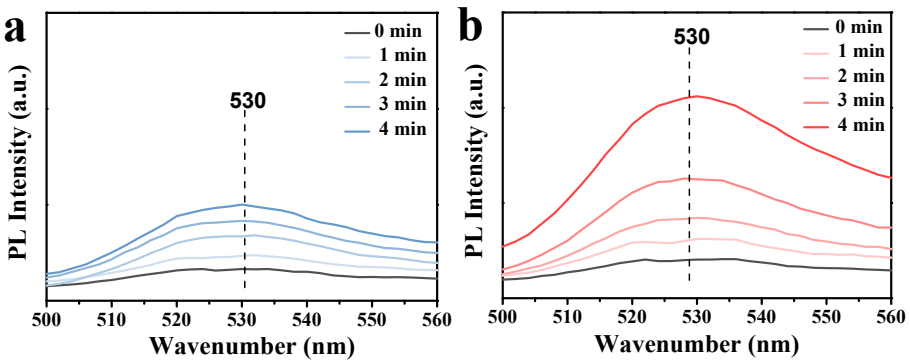

Figure S7. Fluorescence response of 5 μM SOSG recorded during ORR reaction process in the presence of (a) bulk g-C_3N_4 (b) Pt-SA/g-C_3N_4 sheets under 455 nm LED irradiation for 4 min.

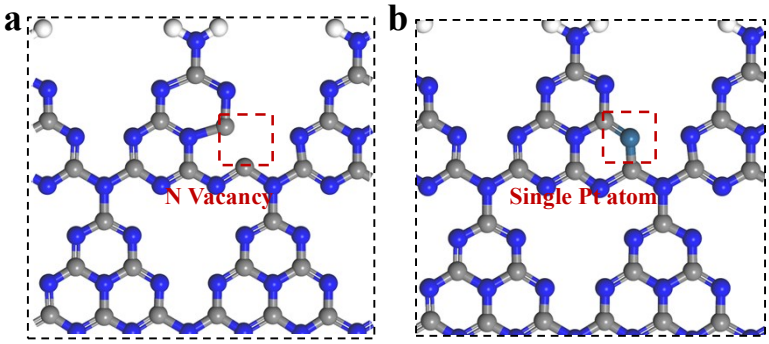

Figure S8. The detail structure of Pt-SA/g-C_3N_4(001) and g-C_3N_4(001).

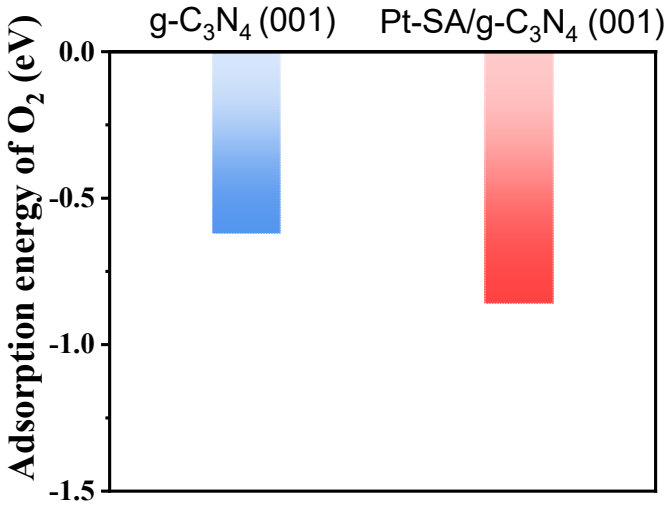

Figure S9. The binding geometries and the corresponding adsorption energies of O_2 on Pt-SA/g-C_3N_4(001) and g-C_3N_4(001).

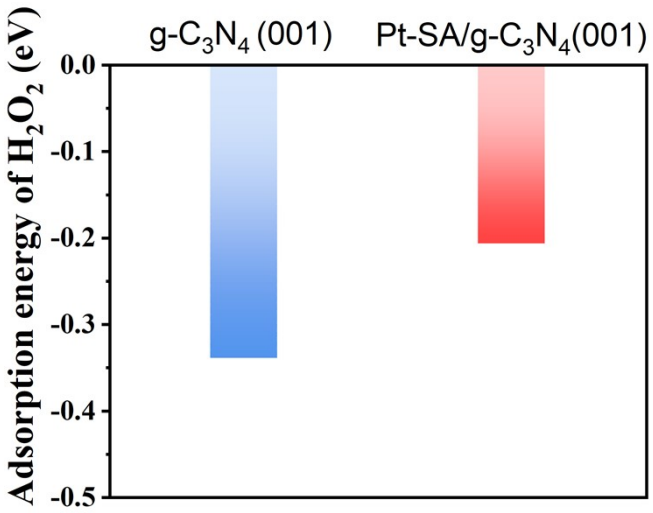

Figure R10. The adsorption energy of H_2O_2 on Pt-SA/g-C_3N_4(001) and on g-C_3N_4(001).

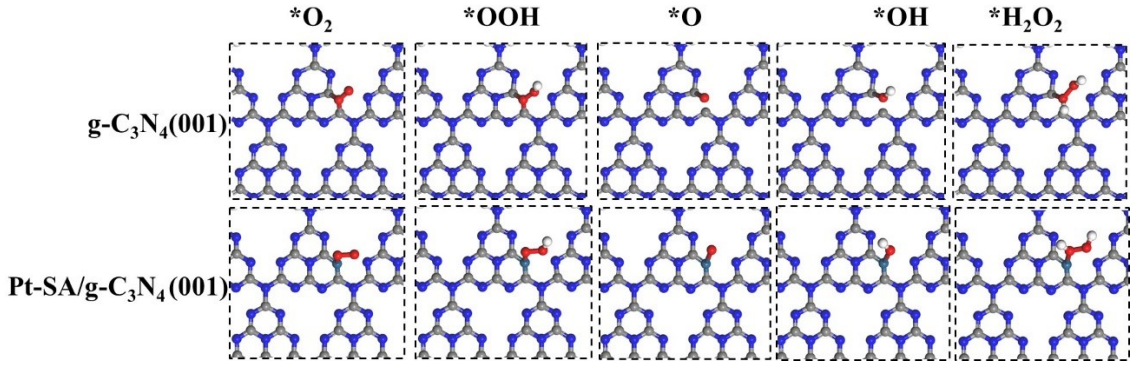

Figure S11. The binding geometries of reaction intermediates on g-C_3N_4(001) and Pt-SA/g-C_3N_4(001).

Table S1. Detailed comparison of visible-light-driven H_2O_2 production from ORR with sacrificial agents based over carbon nitride-based photocatalysts.

Photocatalyst	Experimental conditions				Ref.
	Reaction solution	Gas	Light	μmol·L^{-1}·h^{-1}	
Pt-SA/g-C_3N_4 sheet	20 mg catalyst + 20 mL 20% vol% isopropanol aqueous solution	O_2	6 W blue LED light (455 ±5 nm)	**800**	**This work**
Phosphorus-doped g-C_3N_4 sheet (PCN)	50 mg catalyst + 50 mL 10% vol% ethanol aqueous solution	O_2	9W blue LED (410 nm ≤ λ ≤ 530 nm)	95.11	[7]
Ti_3C_2/ porous g-C_3N_4	50 mg catalyst + 50 mL 10 vol%isopropanol aqueous solution	O_2	300 W Xe lamp (λ > 420 nm)	132	[8]
Anthraquinone-augmented g-C_3N_4	0.5 g L^{-1} catalyst + 10% vol% isopropanol aqueous solution	O_2	150 W Xe lamp (AM 1.5),	180.5	[9]
N vacancy-rich and porous g- C_3N_4	100 mg catalyst + 100 mL 5% methanol aqueous solution	O_2	300 W Xenon lamp (>420 nm)	600	[10]
Heteroatom dopants g-C_3N_4	0.5 g L^{-1} catalyst + 10% ethanol aqueous solution	O_2	300 W Xenon lamp (>420 nm)	683	[11]

porous g-C_3N_4 nanotubes	100 mg catalyst + 100 mL10% ethanol aqueous solution	O_2	300 W Xenon lamp (λ > 420 nm)	93.89	[12]
Nitrogen defect-abundant g-C_3N_4	100 mg catalyst + 100 mL10% ethanol aqueous solution	O_2	300 W Xenon lamp (λ > 420 nm)	283	[13]
Ultrathin g-C_3N_4 nanoplates	30 mg catalyst + 30 mL10% isopropanol aqueous solution	O_2	Visible light illumination (400 nm ⩽ λ ⩽ 700 nm)	43.07	[14]
Hydroxyl-rich g-C_3N_4	50 mg catalyst + 50 mL10% ethanol aqueous solution	O_2	300 W Xenon lamp (λ > 420 nm)	508.4	[15]
Amidation crosslinking polymeric carbon nitride (g-C_3N_4)	10 mg catalyst + 15 mL10% ethanol aqueous solution	O_2	LED light (420 nm)	533	[16]
CoP/g-C_3N_4	20 mg catalyst + 20 mL10% ethanol aqueous solution	O_2	300 W Xe lamp (λ > 420 nm)	70	[17]
NiS@g-C_3N_4	10 mg catalyst + 10 mL10% ethanol aqueous solution	O_2	300 W Xe lamp (λ > 420 nm)	400	[18]
(K, P, O)-g-C_3N_4	20 mg catalyst + 40	O_2	300 W Xe lamp	243	[19]

	mL10% ethanol aqueous solution		(λ > 420 nm)		
polymeric carbon nitride	50 mg catalyst + 50 mL 10% isopropanol aqueous solution	O_2	300 W Xe lamp (λ > 420 nm)	174	[20]
$ZnIn_2S_4$/FTCNso	50 mg catalyst + 100 mL 10% ethanol aqueous solution	O_2	300 W Xe lamp (λ > 420 nm)	136.0	[21]
NH_3-$NaClO_{0.5}$-CNw	100 mg catalyst + 100 mL 10% ethanol aqueous solution	O_2	Xenon lamp (320 nm to 780 nm)	104	[22]
W/CN–SUP	10 mg catalyst + 20 mL 10% ethanol aqueous solution	O_2	Xenon lamp (λ > 400 nm)	161	[23]
NCN-2AP-X	20 mg catalyst + 80 ml 10 vol% triethanolamine aqueous solution	O_2	300 Xenon lamp (λ > 400 nm)	637.5	[24]

References:

[1]. Y. Xiao; G. Tian; W. Li; Y. Xie; B. Jiang; C. Tian; D. Zhao; H. Fu, Molecule Self-Assembly Synthesis of Porous Few-Layer Carbon Nitride for Highly Efficient Photoredox Catalysis, *J. Am. Chem. Soc.* **2019**, *141*, 2508-2515.

[2]. X. Zhang; P. Ma; C. Wang; L. Gan; X. Chen; P. Zhang; Y. Wang; H. Li; L. Wang; X. Zhou, et al., Unraveling the dual defect sites in graphite carbon nitride for ultra-high photocatalytic H_2O_2 evolution, *Energy Environ. Sci.* **2022**, *15*, 830-842.

[3]. R. Ruiz-González; R. Bresolí-Obach; Ò. Gulías; M. Agut; H. Savoie; R. Boyle; S. Nonell; F. Giuntini, NanoSOSG: A Nanostructured Fluorescent Probe for the Detection of Intracellular Singlet Oxygen, *Angew. Chem. Int. Ed.* **2017**, *56*, 2885-2888.

[4]. G.; Joubert Kresse, D., From ultrasoft pseudopotentials to the projector augmented-wave method, *Phys. Rev. B* **1999**, *59*, 1758-1770.

[5]. Burke Perdew , Ernzerhof, Generalized Gradient Approximation Made Simple, *Phys.l Rev. Lett.* **1997**, *77*, 3865-3868.

[6]. G. Stefan; A. Jens; E. Stephan; K. Helge, A consistent and accurate ab initio parametrization of density functional dispersion correction (DFT-D) for the 94 elements H-Pu, *J. Phys. Chem.* **2010**, *132*, 154104.

[7]. D. Li; C. Wen; J. Huang; J. Zhong; P. Chen; H. Liu; Z. Wang; Y. Liu; W. Lv; G. Liu, High-efficiency ultrathin porous phosphorus-doped graphitic carbon nitride nanosheet photocatalyst for energy production and environmental remediation, *Appl. Catal., B* **2022**, *307*, 121099.

[8]. Y. Yang; Z. Zeng; G. Zeng; D. Huang; R. Xiao; C. Zhang; C. Zhou; W. Xiong; W. Wang; M. Cheng, et al., Ti_3C_2 Mxene/porous g-C_3N_4 interfacial Schottky junction for boosting spatial charge separation in photocatalytic H_2O_2 production, *Appl. Catal., B* **2019**, *258*, 117956.

[9]. H. Kim; Y. Choi; S. Hu; W. Choi; J. Kim, Photocatalytic hydrogen peroxide production by anthraquinone-augmented polymeric carbon nitride, *Appl. Catal., B* **2018**, *229*, 121-129.

[10]. Y. Wang; D. Meng; X. Zhao, Visible-light-driven H_2O_2 production from O_2 reduction with nitrogen vacancy-rich and porous graphitic carbon nitride, *Appl. Catal., B* **2020**, *273*, 119064.

[11]. P. Zhang; Y. Tong; Y. Liu; J. Vequizo; H. Sun; C. Yang; A. Yamakata; F. Fan; W. Lin; X. Wang, et al., Heteroatom Dopants Promote Two-Electron O_2 Reduction for

Photocatalytic Production of H_2O_2 on Polymeric Carbon Nitride, *Angew. Chem. Int. Ed.* **2020**, *59*, 16209-16217.

[12]. Y. Song; C. Zhou; Z. Zheng; P. Sun; Y. She; F. Huang; Z. Mo; J. Yuan; H. Li; H. Xu, Porous carbon nitride nanotubes efficiently promote two-electron O_2 reduction for photocatalytic H_2O_2 production, *J. Alloy. Compd.* **2023**, *934*, 167901.

[13]. J. Tian; B. Feng; X. Zhang; K. Gu; Y. Pei; M. Qiao; J. Zhang; B. Zong, One-step nitrogen defect engineering of polymeric carbon nitride for visible light-driven photocatalytic O_2 reduction to H_2O_2, *J. Colloid Inter. Sci.* **2023**, *634*, 138-147.

[14]. W. Liu; C. Song; M. Kou; Y. Wang; Y. Deng; T. Shimada; L. Ye, Fabrication of ultra-thin g-C_3N_4 nanoplates for efficient visible-light photocatalytic H_2O_2 production via two-electron oxygen reduction, *Chem. Eng. J.* **2021**, *425*, 130615.

[15]. Q. Chen; C. Lu; B. Ping; G. Li; J. Chen; Z. Sun; Y. Zhang; Q. Ruan; L. Tao, A hydroxyl-induced carbon nitride homojunction with functional surface for efficient photocatalytic production of H_2O_2, *Appl. Catal., B* **2023**, *324*, 122216.

[16]. Q. Hu; Y. Dong; K. Ma; X. Meng; Y. Ding, Amidation crosslinking of polymeric carbon nitride for boosting photocatalytic hydrogen peroxide production, *J. Catal.* **2022**, *413*, 321-330.

[17]. Y. Peng; L. Wang; Y. Liu; H. Chen; J. Lei; J. Zhang, Visible-Light-Driven Photocatalytic H_2O_2 Production on g-C_3N_4 Loaded with CoP as a Noble Metal Free Cocatalyst, *Eur. J. Inorg. Chem.* **2017**, *2017*, 4797-4802.

[18]. L. Chen; Z. Yang; B. Chen, Uniformly Dispersed Metal Sulfide Nanodots on g-C_3N_4 as Bifunctional Catalysts for High-Efficiency Photocatalytic H_2 and H_2O_2 Production under Visible-Light Irradiation, *Energy Fuels* **2021**, *35*, 10746-10755.

[19]. Gun-hee Moon; Mamoru Fujitsuka; Sooyeon Kim; Tetsuro Majima; Xinchen Wang; Wonyong Choi, Eco-Friendly Photochemical Production of H2O2 through O2 Reduction over Carbon Nitride Frameworks Incorporated with Multiple Heteroelements, *ACS Catal.* **2017**, *7*, 2886-2895.

[20]. Yang Yang; Guangming Zeng; Danlian Huang; Chen Zhang; Donghui He; Chengyun Zhou; Wenjun Wang; Weiping Xiong; Xiaopei Li; Bisheng Li, et al., Molecular engineering of polymeric carbon nitride for highly efficient photocatalytic oxytetracycline degradation and H2O2 production, *Appl. Catal., B* **2020**, *272*.

[21]. Qinghua Liang; Xiaojuan Liu; Binbin Shao; Lin Tang; Zhifeng Liu; Wei Zhang; Shanxi Gong; Yang Liu; Qingyun He; Ting Wu, et al., Construction of fish-scale

tubular carbon nitride-based heterojunction with boosting charge separation in photocatalytic tetracycline degradation and H2O2 production, *Chem. Eng. J.* **2021**, *426*, 130831.

[22]. Yanlin Zhu; Yanyan Sun; Javid Khan; Heng Liu; Guangling He; Xuetao Liu; Jiamin Xiao; Haijiao Xie; Lei Han, NaClO-induced sodium-doped cyano-rich graphitic carbon nitride nanosheets with nitrogen vacancies to boost photocatalytic hydrogen peroxide production, *Chem. Eng. J.* **2022**, *443*, 136501.

[23]. Milad Jourshabani; Seol–Hwa Yun; Mahdieh Razi Asrami; Byeong–Kyu Lee, Superior photodegradation of organic compounds and H2O2 production over tungsten oxide/carbon nitride heterojunction with sizable heptazine units: Dual polycondensation and interface engineering, *Chem. Eng. J.* **2022**, *427*, 131710.

[24]. Baoqian Ye; Hua Tang; Qinqin Liu; Weikang Wang; Lele Wang; Jie Hu, Extended π-conjugated system in carbon nitride by incorporating pyridine rings and N vacancies for photocatalytic H2 evolution and H2O2 production, *Carbon* **2023**, *204*, 465-474.